Taylor & Francis
Taylor & Francis Group

Biofouling
The Journal of Bioadhesion and Biofilm Research

ISSN: 0892-7014 (Print) 1029-2454 (Online) Journal homepage: www.tandfonline.com/journals/gbif20

Aggregation and biofilm formation of mono- and co-culture *Candida* species and *Staphylococcus aureus* are affected by nutrients in growth media

Wan NurHazirah Wan Ahmad Kamil , Mukarramah Zainal , Munirah Mokhtar , H. M. H. N. Bandara , Stuart G. Dashper & Mohd Hafiz Arzmi

To cite this article: Wan NurHazirah Wan Ahmad Kamil , Mukarramah Zainal , Munirah Mokhtar , H. M. H. N. Bandara , Stuart G. Dashper & Mohd Hafiz Arzmi (18 Jun 2025): Aggregation and biofilm formation of mono- and co-culture *Candida* species and *Staphylococcus aureus* are affected by nutrients in growth media, Biofouling, DOI: 10.1080/08927014.2025.2518281

To link to this article: https://doi.org/10.1080/08927014.2025.2518281

Published online: 18 Jun 2025.

BIOFOULING
https://doi.org/10.1080/08927014.2025.2518281

Taylor & Francis
Taylor & Francis Group

Aggregation and biofilm formation of mono- and co-culture *Candida* species and *Staphylococcus aureus* are affected by nutrients in growth media

Wan NurHazirah Wan Ahmad Kamil[a,b,c], Mukarramah Zainal[a,b,c], Munirah Mokhtar[d], H. M. H. N. Bandara[e], Stuart G. Dashper[f] and Mohd Hafiz Arzmi[a,b,f]

[a]Department of Fundamental Dental and Medical Sciences, Kulliyyah of Dentistry, International Islamic University Malaysia, Kuantan, Pahang, Malaysia; [b]Cluster of Cancer Research Initiative IIUM (COCRII), International Islamic University Malaysia, Kuantan, Pahang, Malaysia; [c]Faculty of Dentistry, Universiti Teknologi MARA (UiTM), Sungai Buloh, Selangor, Malaysia; [d]Department of Medical Diagnostic, Universiti Selangor, Malaysia; [e]Bristol Dental School, University of Bristol, Bristol, United Kingdom; [f]Melbourne Dental School, The University of Melbourne, Victoria, Australia

ABSTRACT

Candida species and *Staphylococcus aureus* coexist in nosocomial infections. These interkingdom interactions are associated with oral biofilm formation, leading to various oral diseases. This study elucidated the interkingdom interactions of these microorganisms, particularly their aggregation and biofilm formation, in three different media. *Candida auris, Candida albicans, Candida lusitaniae, Candida dubliniensis, Candida parapsilosis, Candida glabrata* and *S. aureus* were used in this study. Aggregation assays were conducted to determine planktonic interaction, and biofilm assays were performed to investigate intra- and interkingdom interactions in a static biofilm environment. Most *Candida* spp. exhibited a high auto-aggregation percentage in brain heart infusion broth supplemented with yeast extract (BHIYE). In addition, co-culture biofilm with *S. aureus* significantly reduced the total cell counts of *Candida* spp. compared to mono-culture ($p < 0.05$). In conclusion, co-aggregation, biofilm biomass and total cell count were species- and growth medium-dependent, and *S. aureus* interacted antagonistically with *Candida* spp.

ARTICLE HISTORY
Received 15 November 2024
Accepted 30 May 2025

KEYWORDS
Interkingdom interactions; co-infections; growth media; aggregation; biofilm; Candida

Introduction

The human oral cavity provides a habitat for the oral microbiome. This complex oral microbiome comprises interconnected communities, including those formed by yeast and bacteria (Deo and Deshmukh 2019; Sharma et al. 2023). Communication among microbes, such as direct cell-to-cell interactions *via* chemical signals and metabolic cooperation, leads to the formation of microbial biofilms (Deo and Deshmukh 2020). During the formation of interkingdom biofilms, yeast and bacteria engage in both physical and chemical interactions. These interactions include aggregation and cell-to-cell signalling (Wimpenny 2009; Palencia et al. 2022). Various bidirectional communications and regulatory mechanisms tightly regulate the oral microbiome and host responses, ensuring host-microbial homeostasis and promoting oral health. Dysbiotic alterations in the oral microbiome can result in oral diseases, including caries, periodontal disease, oral candidiasis and other opportunistic infections. It is now well-known that the microbial interactions within the biofilms contribute to initiating and aggravating dysbiotic relationships in the oral microbiota (Lamont et al. 2018).

The interest in the research on interkingdom interactions among oral microbiota in biofilm communities is increasing. Approximately half of the human population carries *Candida* species in their oral cavity as a commensal organism. In susceptible individuals, *Candida* spp. can cause mild to severe life-threatening infections (Cortegiani et al. 2019). *Candida* spp. also colonises the gut, skin, respiratory tract, genitourinary tract and even medical devices. Among these, *Candida albicans*, *Candida auris*, *Candida glabrata* (*Nakaseomyces glabrata*), *Candida parapsilosis* and *Candida dubliniensis* are frequently isolated as significant human fungal pathogens (Papon et al. 2013; Bayraktar et al. 2017; Farooq et al. 2022; Kidd et al. 2023). Importantly, the World Health Organisation (WHO) has categorised *C. albicans* and *C. auris* as critical priority pathogens in the Fungal Priority Pathogens List. This classification is due to their ability to induce aggressive acute and subacute systemic fungal infections, which complicate drug treatment

CONTACT Mohd Hafiz Arzmi hafizarzmi@iium.edu.my

and clinical management (Parums 2022). Meanwhile, *C. parapsilosis* and *C. glabrata* were categorised under high-priority pathogens in the Fungal Priority Pathogens List (Parums 2022).

Staphylococcus aureus is a bacterial pathogen of worldwide concern, which could cause serious nosocomial and community-acquired infections. The bacterium is listed among the high-priority pathogens by the WHO due to the prevalence of severe infections and the rise of antibiotic-resistant strains (Sati et al. 2025). Studies have also reported that oral biofilms colonised with *Candida* spp. and *S. aureus* lead to various oral pathologies, including dental caries, periodontal diseases, peri-implantitis, oral candidiasis, mucosal lesions (such as leukoplakia, lichen planus) and oral cancer (Carolus et al. 2019; Di Cosola et al. 2021; Huang et al. 2023).

Candida-bacteria interactions play a key role in mediating the colonisation of *Candida* spp. in the oral environment (Eichelberger et al. 2023). The interaction between *Candida* spp. and *S. aureus* raises concerns due to their virulence and resistance to treatment in nosocomial infection. Previous studies have reported that *C. albicans* interacts with bacteria found in the oral cavity (Gülmez et al. 2022). *C. albicans*, *C. auris* and *S. aureus* are the most common pathogens linked to hospital-acquired infections. Co-infections involving these pathogens often worsen patient prognosis (Carolus et al. 2019). However, the effect of nutrients on interkingdom interactions of *S. aureus* with non-albicans *Candida* species (NAC), particularly *C. auris*, *C. glabrata*, *C. parapsilosis* and *C. dubliniensis* remains limited.

Furthermore, this is the first study reported on the effects of nutrients on the interkingdom interaction between the nosocomial infection *C. auris* and *S. aureus* in both planktonic and biofilm environments, using *C. albicans* as the reference strain. Addressing these gaps could pave to new therapeutic strategies that target co-infections and improve outcomes for those affected patients. Therefore, this research aimed to elucidate the impact of nutrients in the growth medium on the aggregation and biofilm development of *Candida* spp. and *S. aureus* in mono- and co-culture environments. It is hypothesised that aggregation and biofilm formation are medium and species-dependent.

Materials and methods

Growth of microorganisms

The microbial strains utilised in this study included *C. albicans* (ALC2) isolated from oral sample of an AIDS patient, *C. auris* (ATCC MYA-5002), *Candida lusitaniae* (ATCC 64215), *C. dubliniensis* (ATCC MYA-2975), *C. parapsilosis* (ATCC 22019), *C. glabrata* (ATCC 90030) and *S. aureus* (ATCC 25923). These microbial strains were supplied by the Cluster of Cancer Research Initiative IIUM (COCRII), Kulliyyah of Dentistry, International Islamic University Malaysia. *Candida* spp. were subcultured onto yeast peptone dextrose (YPD) agar (Difco, Tampa, FL, USA). Meanwhile, *S. aureus* (ATCC 25923) was inoculated onto brain heart infusion (BHI) agar (Difco, Tampa, FL, USA). The plates underwent aerobic incubation at 37 °C for 24 h.

Auto- and co-aggregation assay

Candida spp. and *S. aureus* were inoculated separately to evaluate auto-aggregation and concurrently to evaluate co-aggregation (Mokhtar et al. 2021). Initially, *Candida* spp. were grown in three different media to assess nutrient-dependent interactions: RPMI-1640 (Gibco™, Thermo Fisher Scientific, Waltham, MA, USA) (to mimic host-like conditions), YPD (for optimal fungal growth) and brain heart infusions supplemented with yeast extract (BHIYE) (Difco, Tampa, FL, USA) broth to support co-culture with *S. aureus*. BHIYE is a nutrient-rich medium that supports both bacteria and fungal growth due to its high content of peptones, proteins, B-complex vitamins and yeast extract. It was prepared by dissolving 37 g of the BHI powder and adding 5 g of yeast extract in 1 l of distilled water (Moore and McMullan 2003). The mixture was then autoclaved at 121 °C for 15 min. These media were selected based on their varying nutrient profiles, enabling the evaluation of aggregation and biofilm formation under resource-limited, fungal-optimised and interkingdom-supportive environments.

The inocula were cultured to stationary phase by incubating them for 24 h at 37 °C in aerobic condition. The cells were obtained by centrifuging at 12,000 g for 5 min and subsequently washed two times with co-aggregation buffer consisting of 0.1 mM $CaCl_2$, 0.1 mM $MgCl_2$, 150 mM NaCl and 3.1 mM NaN_3 in 1 mM Tris buffer, adjusted to pH 7.0. The supernatant was removed, and the pellet was re-suspended in the co-aggregation buffer. For *S. aureus*, the same method was used by substituting the media with BHI broth.

To evaluate auto-aggregation, each *Candida* spp. and *S. aureus* were standardised in a co-aggregation buffer to achieve final cell densities of 10^6 cells ml^{-1}

and 10^7 cells ml^{-1}, respectively, in distinct sterile 2 ml Eppendorf tubes. This corresponds to an optical density of 0.5 at a wavelength of 620 nm (OD_{620nm}). A vortex mixer thoroughly mixed each suspension for 30 s, and the OD_{620nm} at the time (t) = 0 h was measured. The inoculum was left at room temperature for 1 h to facilitate aggregation, and the OD_{620nm} was documented. A sterile co-aggregation buffer was used as the standard blank. A similar method was used to assess co-aggregation by inoculating individual *Candida* spp. and *S. aureus* into the same 2 ml Eppendorf tube. The percentages of auto- and co-aggregation were assessed using the following equation:

The calculation for percentage aggregation was done using this equation:

$$\%\ \text{Auto} - \text{ or co} - \text{aggregation} = \left(\left[OD_{620nm}(t = 0\ h) - OD_{620nm}(t = 1\ h)\right] / OD_{620nm}(t = 0\ h)\right) \text{ x } 100$$

The percentage of co-aggregation was classified into three categories: increased, maintained and decreased aggregation scores compared to auto-aggregation scores.

Morphological observation

The study employed the method outlined by Mokhtar et al. (2021) to evaluate the morphological characteristics of *Candida* spp. during auto- and co-aggregation processes. In brief, following the aggregation assay, 100 µl of the suspension was pipetted onto a glass slide and left to dry for 10 min. The slide was stained using a 0.1% (w/v) crystal violet solution. The cell aggregation was then observed using a light microscope.

Mono and co-culture biofilm assay

Following the methodology outlined by Arzmi et al. (2023). Single colonies of *Candida* spp. were re-suspended in RPMI-1640, YPD, or BHIYE broth to assess mono-culture biofilm. The inocula were standardised to achieve a cell density of 10^6 cells ml^{-1}. Meanwhile, *S. aureus* was re-suspended in BHI broth and standardised to 10^7 cells ml^{-1}. These cell densities were equivalent to an absorbance of 0.5 at OD_{620nm} in a separate 2 ml Eppendorf tube. Next, 60 µl of the suspension comprising 6×10^5 cells of *Candida* spp. or 6×10^6 cells of *S. aureus* was pipetted into a separate well of a sterile 96-well plate. Later, 120 µl of RPMI-1640, YPD, or BHIYE broth was placed into each well, resulting in a total volume of 180 µl. The 96-well plate underwent incubation for 72 h at 37 °C to facilitate biofilm maturation (Mokhtar et al. 2021) The culture medium was replaced aseptically every 24 h during this process. A similar method was used to investigate the biofilm formation in co-culture by inoculating *Candida* spp. and *S. aureus* into the same well of 96-well plates.

Determination of biofilm biomass using crystal violet assay

Crystal violet (CV) assay was conducted following the methodology described by Arzmi et al. (2023). The non-adherent cells were removed by rinsing the biofilm two times with sterile phosphate-buffered saline (PBS) (Gibco™, Thermo Fisher Scientific, Waltham, MA, USA). Next, 200 µl of methanol was added to each well for fixation, followed by a 15 min incubation at 25 °C. The supernatant was removed, and the sample was left to dry for 45 min. Later, 200 µl of 0.1% (w/v) CV (Sigma-Aldrich, St. Louis, MO, USA) solution was placed into each well and incubated at 25 °C for 20 min. The sample was thoroughly washed two times with running tap water. Then, 200 µl of 33% (v/v) acetic acid was pipetted into each well to de-stain the biofilm.

The plate was kept at room temperature for 5 minutes. Then, 100 µl of the suspension was pipetted into a new sterile 96-well plate. Absorbance was recorded at OD_{620nm} with a microtiter plate reader (Victor3, Perkin-Elmer, Waltham. MA, USA).

Analysis of total cell count for *Candida* spp.

After developing the biofilm, each well was scraped mechanically with a sterile pipette tip to remove the biofilm. Following that, 100 µl of the aliquot was transferred into a 2 ml microcentrifuge tube containing 900 µl of PBS. Lastly, 10 µl of the diluted inoculum was placed in a haemocytometer to quantify *Candida* spp. total cell count (Mokhtar et al. 2021).

Aggregation and biofilm morphology observation

The morphology of auto- and co-aggregation was examined using a CH Series Light Microscope (Olympus, BX53, Japan) using the method described in the 'Morphological observation' section.

Statistical analysis

All data were analysed using GraphPad Prism software v10.0. An independent t-test was conducted to compare the auto- and co-aggregation of *Candida* spp. in RPMI-1640, YPD and BHIYE. One-way analysis of variance (ANOVA) associated with *post hoc* Tukey's test was conducted to compare biofilm biomass and total cell count between *Candida* spp. in mono- and co-culture biofilms. The data were considered statistically significant when $p < 0.05$. Each experiment involved three independent biological replicates, with each replicate comprising three technical replicates.

Results

Auto-aggregation and co-aggregation

Different *Candida* spp. varied in auto-aggregation scores in three media: RPMI-1640, YPD and BHIYE (Table 1). The auto-aggregation scores ranged from 0.17 ± 0.04% (*C. dubliniensis* in BHIYE) to 2.87 ± 0.02% (*C. auris* in BHIYE). *C. auris* demonstrated the highest auto-aggregation score in YPD and BHIYE. Meanwhile, *C. glabrata* exhibited the highest auto-aggregation score in RPMI-1640 (Table 1).

Candida spp. and *S. aureus* co-aggregated in all tested media (RPMI-1640, YPD and BHIYE broth), ranging from 0.13 ± 0.01% (*C. parapsilosis* in BHIYE) to 3.00 ± 0.02% (*C. auris* in BHIYE). The co-aggregation scores of *Candida* spp. and *S. aureus* were categorised as increased, maintained and decreased percentages of co-aggregation compared to auto-aggregation (Table 1). The result showed that the majority of *Candida* spp. exhibited decreased co-aggregation percentages when co-incubated with *S. aureus* in all three media compared to auto-aggregation (Table 1).

However, *C. auris* showed an increased percentage of aggregation when grown with *S. aureus* in BHIYE compared to auto-aggregation (2.87 ± 0.02% to 3.00 ± 0.02%). In addition, *C. albicans,* when co-incubated with *S. aureus* in BHIYE and YPD, showed an increased percentage aggregation compared to auto-aggregation by 1.18 ± 0.01% to 1.36 ± 0.13% and 0.51 ± 0.02% to 0.73 ± 0.01%, respectively. *C. dubliniensis* showed increased aggregation scores when co-cultured in RPMI-1640 (0.34 ± 0.06% to 0.69 ± 0.02%) and YPD (0.18 ± 0.00% to 0.30 ± 0.00%) compared to auto-aggregation. Meanwhile, *C. dubliniensis* (0.17 ± 0.02%) maintained aggregation scores in BHIYE. Overall, co-aggregation of *Candida* spp. and *S. aureus* showed significant differences in all three tested media ($p < 0.05$) (Figure 1).

Morphological observation of Candida spp. and Staphylococcus aurues

The photomicrographs illustrated *Candida* spp. and *S. aureus* co-aggregation grown in BHIYE as observed under a light microscope following 1 h incubation in the co-aggregation buffer (Figure 2). Overall, *Candida* spp. co-aggregate with *S. aureus* in all three tested media, with most bacteria bound to *Candida* yeast form.

Effect of growth media and interkingdom interactions on biofilm biomass

The biofilm biomass is divided into three categories using CV measurement cut-offs: low biofilm biomass

Table 1. Percentage of auto and co-aggregation *Candida* species and *Staphylococcus aureus* in three types of growth media: RPMI-1640, YPD, and BHIYE.

	RPMI-1640		YPD		BHIYE	
Microorganisms	Auto-aggregation (SD)	Co-aggregation (SD)	Auto-aggregation (SD)	Co-aggregation (SD)	Auto-aggregation (SD)	Co-aggregation (SD)
C. auris	2.42 (0.09)	1.86 (0.01)	2.48 (0.02)	2.10 (0.02)	2.87 (0.02)	3.00 (0.02)
C. albicans	0.51 (0.02)	0.73 (0.01)	0.31 (0.05)	0.28 (0.04)	1.18 (0.01)	1.36 (0.13)
C. lusitaniae	0.47 (0.02)	0.25 (0.04)	0.37 (0.08)	0.28 (0.06)	0.70 (0.01)	0.14 (0.09)
C. dubliniensis	0.34 (0.06)	0.69 (0.02)	0.18 (0.00)	0.30 (0.00)	0.17 (0.04)	0.17 (0.02)
C. parapsilosis	0.30 (0.01)	0.23 (0.04)	0.36 (0.03)	0.21 (0.05)	2.45 (0.01)	0.13 (0.01)
C. glabrata	2.61 (0.02)	0.24 (0.06)	0.30 (0.03)	0.13 (0.08)	2.23 (0.03)	0.14 (0.00)

Percentage auto-aggregation and co-aggregation, as measured by OD_{620nm}, changes over 1 h. *S. aureus* was grown in BHI, given the auto-aggregation score of 0.39 ± 0.06. The data represent the means from three biological replicates, with each replicate consisting of three technical replicates ($N = 9$). The standard deviation (SD) is given in parentheses. Auto-aggregation scores represent the interaction between cells from the same kingdom, and co-aggregation scores represent the interkingdom interactions of *Candida* spp. with *S. aureus* in planktonic. Increased ( ), maintained ( ), and decreased ( ) aggregation scores compared to auto-aggregation.

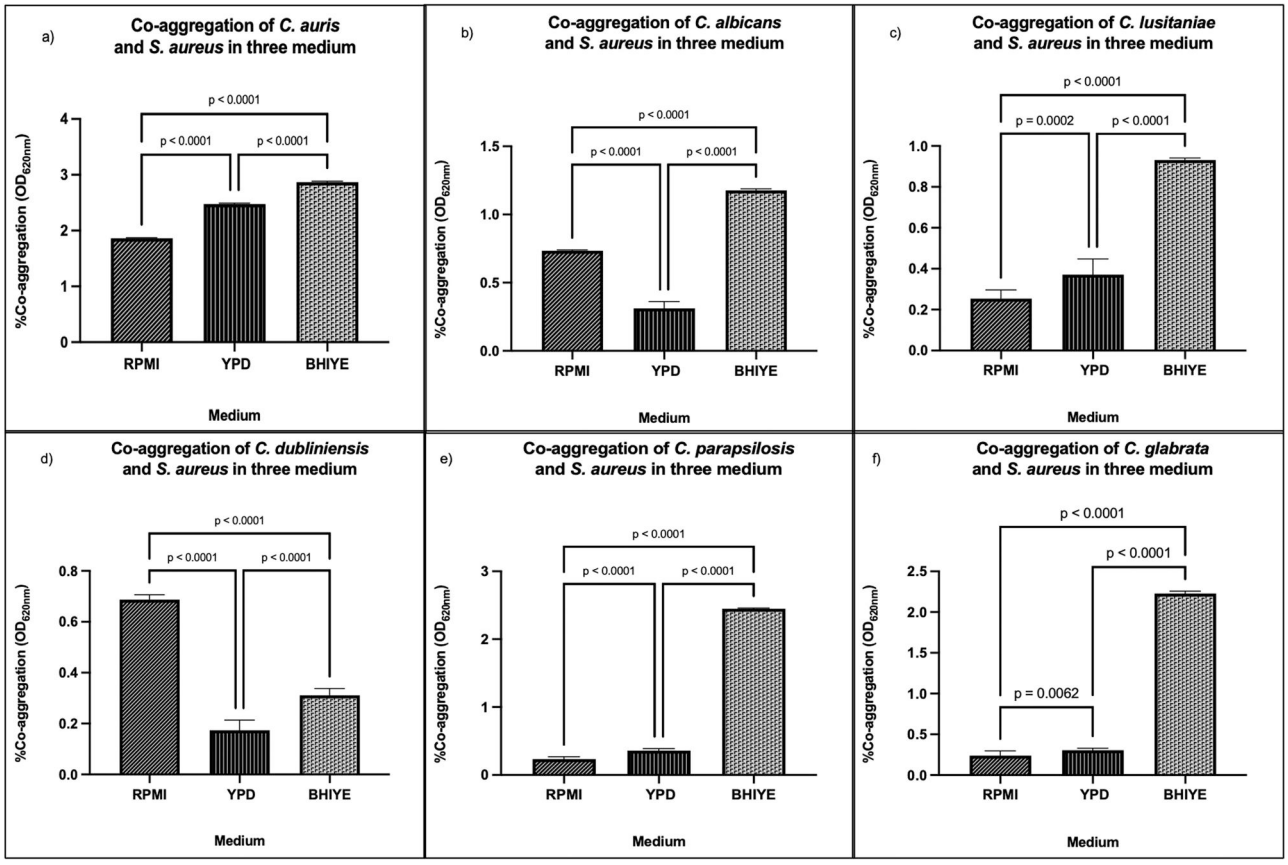

Figure 1. Co-aggregation of *C. auris* ATCC MYA-5002 (a), *C. albicans* ATCC MYA-4901 (b), *C. lusitaniae* ATCC 64215 (c), *C. dubliniensis* ATCC MYA-2975 (d), *C. parapsilosis* ATCC 22019 (e) and *C. glabrata* ATCC 90030 (f) in RPMI-1640, YPD and BHIYE after 1 h in co-aggregation buffer.

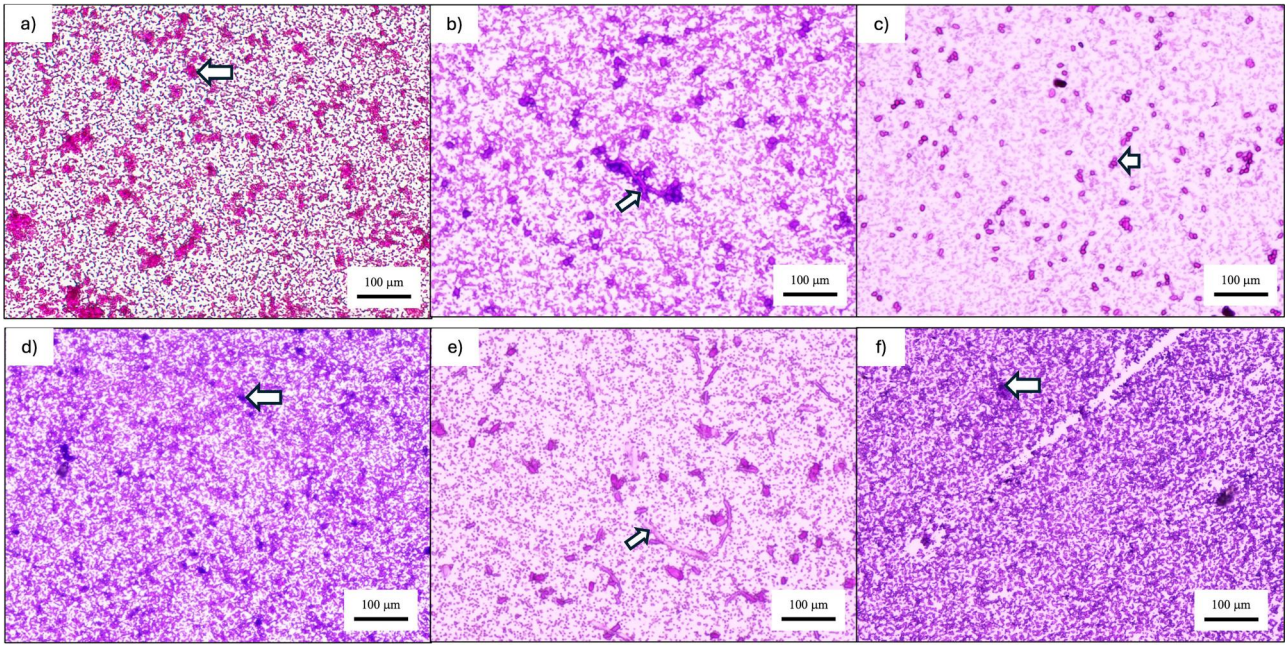

Figure 2. Photomicrographs illustrating the co-aggregation of *S. aureus* and *C. auris* ATCC MYA-5002 (a), *C. albicans* ATCC MYA-4901 (b), *C. lusitaniae* ATCC 64215 (c), *C. dubliniensis* ATCC MYA-2975 (d), *C. parapsilosis* ATCC 22019 (e) and *C. glabrata* ATCC 90030 (f) were grown in BHIYE medium at 40× magnification. The white arrows indicate the dark-stained yeast (a, c, d, and f) and hyphae (b and e) morphologies showing the encapsulation of *Candida* by *S aureus.*

(LBB) < 0.197, moderate biofilm biomass (MBB) 0.197-0.327, high biofilm biomass (HBB) > 0.327 (Marcos-Zambrano et al. 2014; Arzmi et al. 2023) (Table 2). The highest biofilm biomass score was the mono-culture of *C. dubliniensis* in YPD (1.165 ± 0.005), and the lowest biofilm biomass score was the co-culture of *C. lusitaniae* in RPMI-1640 (0.110 ± 0.031).

Mono-culture biofilm biomass scores of all *Candida* spp. varied in all three different media. In YPD, all mono-culture *Candida* spp. exhibited HBB. Among the mono-culture biofilm biomass, YPD-grown *C. dubliniensis* (1.165 ± 0.005) had the highest score, and BHIYE-grown *C. albicans* (0.127 ± 0.000) had the lowest score.

Candida spp. biofilm biomass scores varied in all three media when co-cultured with *S. aureus* (Figure 3). Among the co-culture biofilm biomass, YPD-grown *C. glabrata* (0.929 ± 0.001) had the highest score, followed by *C. albicans* (0.499 ± 0.001) and *C. auris* (0.465 ± 0.001) in BHIYE. Five RPMI-grown *Candida* spp. (*C. auris*, *C. lusitaniae*, *C. dubliniensis*, *C. parapsilosis* and *C. glabrata*) biofilms were LBB when co-cultured with *S. aureus* (Table 2). Overall, the co-culture biofilm of *Candida* spp. and *S. aureus* showed significant differences in all three tested media ($p < 0.05$) (Figure 3).

In addition, three BHIYE-grown (*C. auris*, *C. albicans* and *C. glabrata*) were HBB when grown as co-culture. These co-culture biofilms showed a significant increase in biomass compared to mono-culture *Candida* spp. ($p < 0.05$). Co-cultured *Candida* spp. with *S. aureus* in YPD significantly decreased biofilm biomass scores ($p < 0.05$), except for *C. glabrata*, which significantly increased biofilm biomass scores ($p < 0.05$) compared to mono-culture *Candida* spp. (Table 2).

Effect of growth media and interkingdom interactions on *Candida* spp. cell count

In mono-culture biofilm, *C. auris* in BHIYE recorded the highest cell count ($1.858 \pm 0.02 \times 10^7$ cells ml^{-1}), and the lowest was *C. dubliniensis* in RPMI-1640 ($0.122 \pm 0.001 \times 10^7$ cells ml^{-1})(Table 3). In co-culture biofilms, BHIYE-grown *C. auris* demonstrated the highest total cell count ($0.661 \pm 0.03 \times 10^7$ cells ml^{-1}), followed by *C. albicans* ($0.586 \pm 0.001 \times 10^7$ cells ml^{-1} (Table 3). The total cell count of *Candida* spp. was significantly decreased when co-cultured with *S. aureus* compared to mono-culture biofilm ($p < 0.05$; Table 3). Overall, the total cell count of *Candida* spp. in the co-culture biofilm showed significant differences in all three tested media ($p < 0.05$) (Figure 4).

Morphological observation of Candida spp. and Staphylococcus aureus biofilm

The photomicrographs illustrated the mono- (Figures 5-7) and co-culture (Figures 8-10) biofilms of *Candida* spp. in BHIYE, RPMI-1640 and YPD medium. In a co-culture biofilm, *C. albicans* ATCC MYA-4901 (Figure 8b) and *C. parapsilosis* ATCC 22019 (Figure 10e) were found to develop more hyphae compared to the mono-culture condition (Figures 8–10). Overall, the morphology of *Candida*

Table 2. Scores for biofilm biomass of six *Candida* spp. and *Staphylococcus aureus* grown as mono- and co-culture biofilms after 72 h incubation in three types of growth media: RPMI-1640, YPD, and BHIYE.

	RPMI-1640		YPD		BHIYE	
Species	Monoculture (SD)	Co-culture (SD)	Monoculture (SD)	Co-culture (SD)	Monoculture (SD)	Co-culture (SD)
C. auris	0.197 (0.010)	0.115* (0.009)	0.445 (0.002)	0.348* (0.016)	0.270 (0.001)	0.465* (0.017)
C. albicans	0.296 (0.04)	0.244* (0.040)	0.426 (0.032)	0.163* (0.036)	0.127 (0.000)	0.499* (0.001)
C. lusitaniae	0.132 (0.023)	0.110 (0.031)	0.350 (0.042)	0.227* (0.020)	0.175 (0.030)	0.325* (0.001)
C. dubliniensis	0.205 (0.018)	0.114* (0.035)	1.165 (0.005)	0.327* (0.007)	0.315 (0.02)	0.153* (0.00)
C. parapsilosis	0.205 (0.007)	0.126* (0.002)	1.004 (0.033)	0.298* (0.017)	0.370 (0.017)	0.203* (0.000)
C. glabrata	0.128 (0.011)	0.141 (0.051)	0.906 (0.005)	0.929* (0.001)	0.177 (0.013)	0.329* (0.087)
S. aureus	0.369 (0.068)		0.236 (0.016)		0.333 (0.002)	

Absorbance was measured at wavelength OD_{620nm} after 72 h incubation. The data are means of three biological replicates, with each replicate consisting of three technical replicates ($N = 9$). The standard deviations (SD) are given in parentheses. Significant differences ($p < 0.05$) were observed between co-cultured *Candida* spp. with *S. aureus* (*) compared to mono-cultured *Candida* spp. biofilms. Data was categorised as low biofilm biomass ( ), moderate biofilm biomass ( ) and high biofilm biomass ( ).

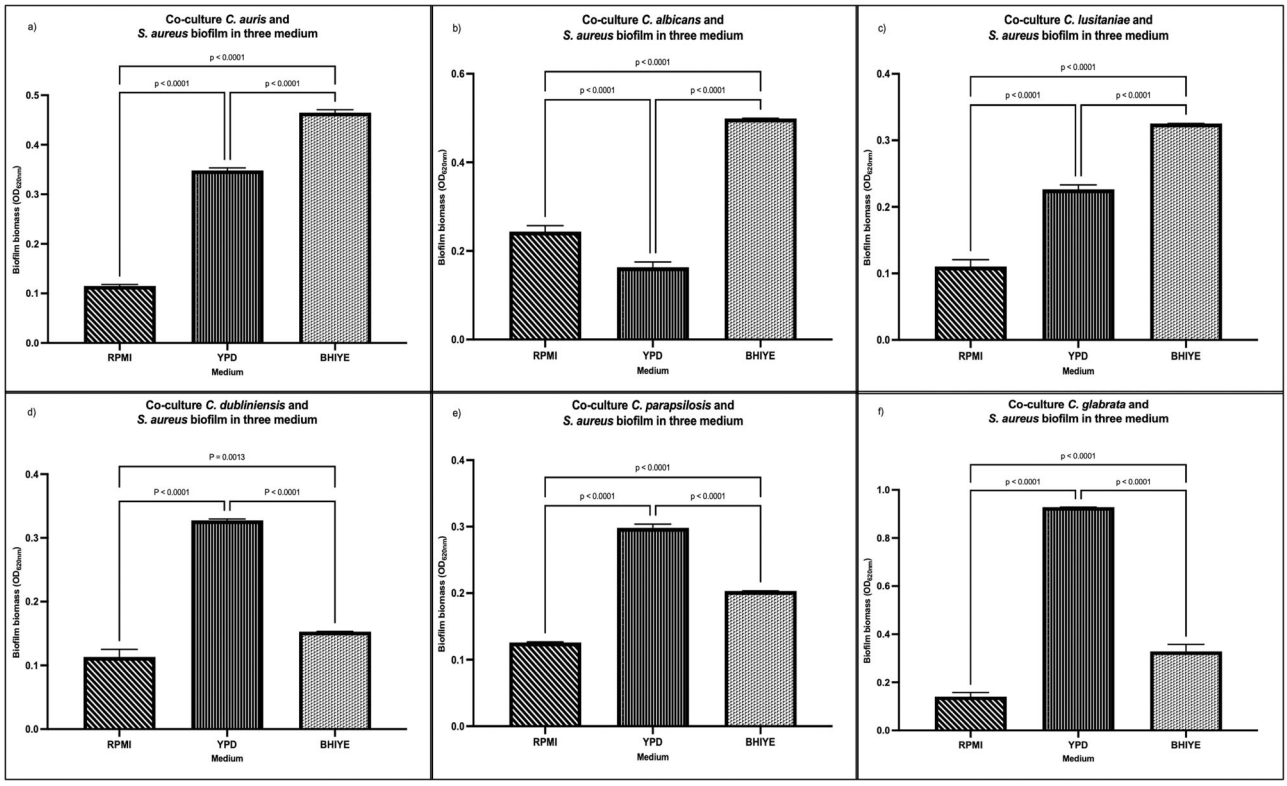

Figure 3. Biofilm biomass score of co-culture *C. auris* ATCC MYA-5002 (a), *C. albicans* ATCC MYA-4901 (b), *C. lusitaniae* ATCC 64215 (c), *C. dubliniensis* ATCC MYA-2975 (d), *C. parapsilosis* ATCC 22019 (e) and *C. glabrata* ATCC 90030 (f) grown in RPMI-1640, YPD, and BHIYE after 72 h incubation.

Table 3. Total cell counts of *Candida* species in mono- and co-culture biofilms with *Staphylococcus aureus* after 72 h incubation in three types of growth media: RPMI-1640, YPD, and BHIYE.

	Total cell count (x 10^7 cells ml^{-1})					
	RPMI-1640		YPD		BHIYE	
Species	Monoculture (SD)	Co-culture (SD)	Monoculture (SD)	Co-culture (SD)	Monoculture (SD)	Co-culture (SD)
C. auris	1.655 (0.001)	0.421* (0.026)	1.236 (0.104)	0.557* (0.001)	1.858 (0.002)	0.661* (0.029)
C. albicans	1.537 (0.011)	0.341* (0.019)	1.254 (0.016)	1.139* (0.012)	1.736 (0.002)	0.586* (0.001)
C. lusitaniae	0.230 (0.006)	0.122* (0.009)	0.550 (0.101)	0.322* (0.009)	0.360 (0.035)	0.244* (0.027)
C. dubliniensis	0.122 (0.001)	0.102* (0.001)	0.133 (0.006)	0.108* (0.002)	0.130 (0.015)	0.108* (0.005)
C. parapsilosis	0.618 (0.001)	0.437* (0.055)	0.766 (0.009)	0.448* (0.086)	0.850 (0.030)	0.635* (0.002)
C. glabrata	0.329 (0.001)	0.215* (0.005)	0.442 (0.010)	0.419 (0.083)	0.469 (0.031)	0.326* (0.001)

Data are expressed as cell counts per millilitre (cells ml^{-a}) and are the means of three separate experiments ($N = 3$). The standard deviation (SD) is given in parentheses. Significant differences ($p < 0.05$) were observed in total cell counts between co-cultured *Candida* spp. with *S. aureus* (*) compared to mono-cultured *Candida* spp. biofilms.

spp. is yeast form either mono or co-culture condition in all three tested media (Figures 5–10).

Discussion

The interaction between *Candida* spp. and *S. aureus* is critical for microbiome pathogenesis, including aggregation and biofilm formation (Chantanawilas et al. 2024). These interactions can influence the severity of oral infections and their therapeutic management (Eichelberger et al. 2023). In addition, oral biofilms of *Candida* spp. especially *C. albicans, C. auris, C. parapsilosis* and *C. glabrata* have been linked with considerably high hospital morbidity and mortality (Vitális et al. 2020).

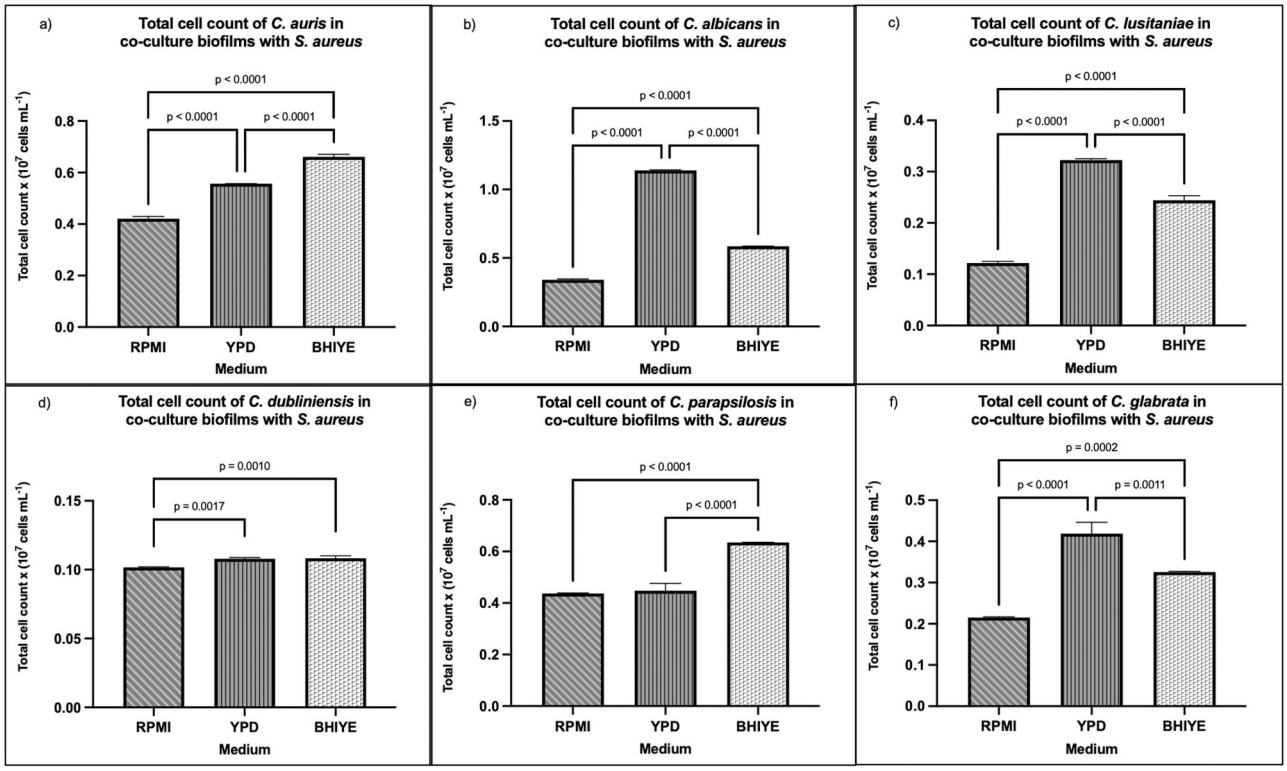

Figure 4. Total cell count of *C. auris* ATCC MYA-5002 (a), *C. albicans* ATCC MYA-4901 (b), *C. lusitaniae* ATCC 64215 (c), *C. dubliniensis* ATCC MYA-2975 (d), *C. parapsilosis* ATCC 22019 (e) and *C. glabrata* ATCC 90030 (f) in co-culture biofilms grown in RPMI-1640, YPD and BHIYE after 72 h incubation.

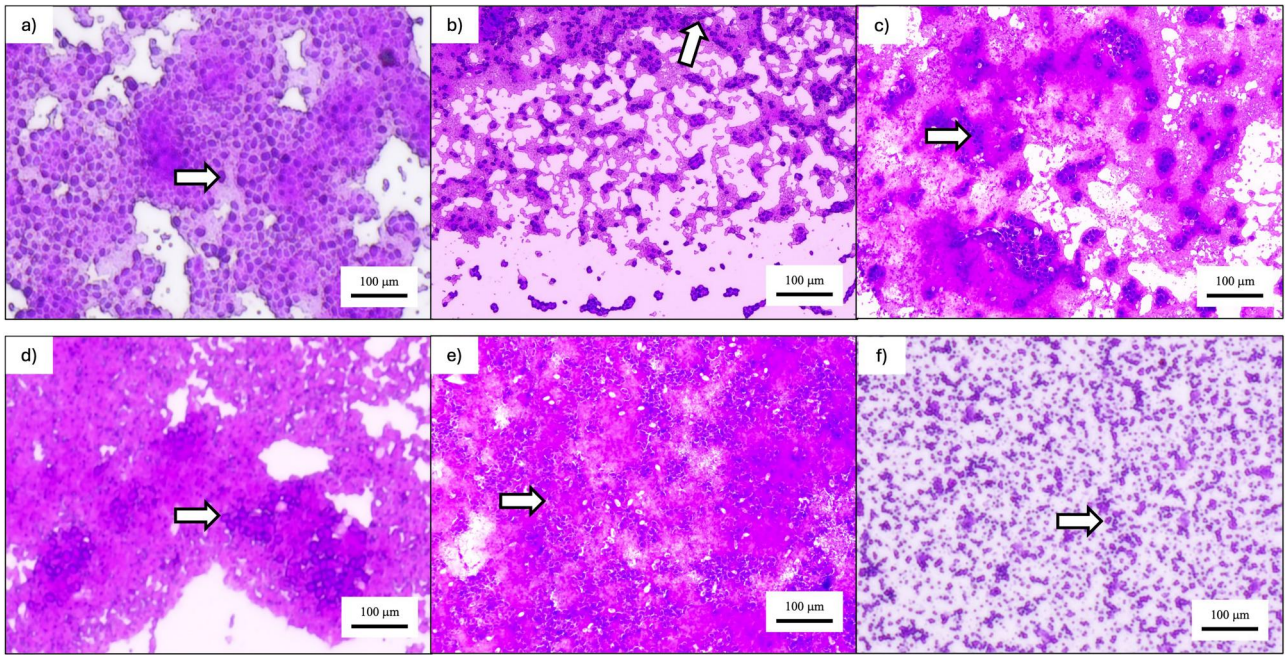

Figure 5. Photomicrographs illustrating the mono-culture biofilms of *C. auris* ATCC MYA-5002 (a), *C. albicans* ATCC MYA-4901 (b), *C. lusitaniae* ATCC 64215 (c), *C. dubliniensis* ATCC MYA-2975 (d), *C. parapsilosis* ATCC 22019 (e) and *C. glabrata* ATCC 90030 (f) at 40× magnification. Biofilms grown in BHIYE for 72 h at 37 °C. The white arrows indicate the morphology of *Candida* yeast.

This study demonstrated that the growth media significantly influence both aggregation and biofilm formation due to the varying nutrient availability in the oral cavity environment. In oral settings, nutrient availability exists within saliva-coated mucosal surfaces and carbohydrate-rich dental plaque tissues. This

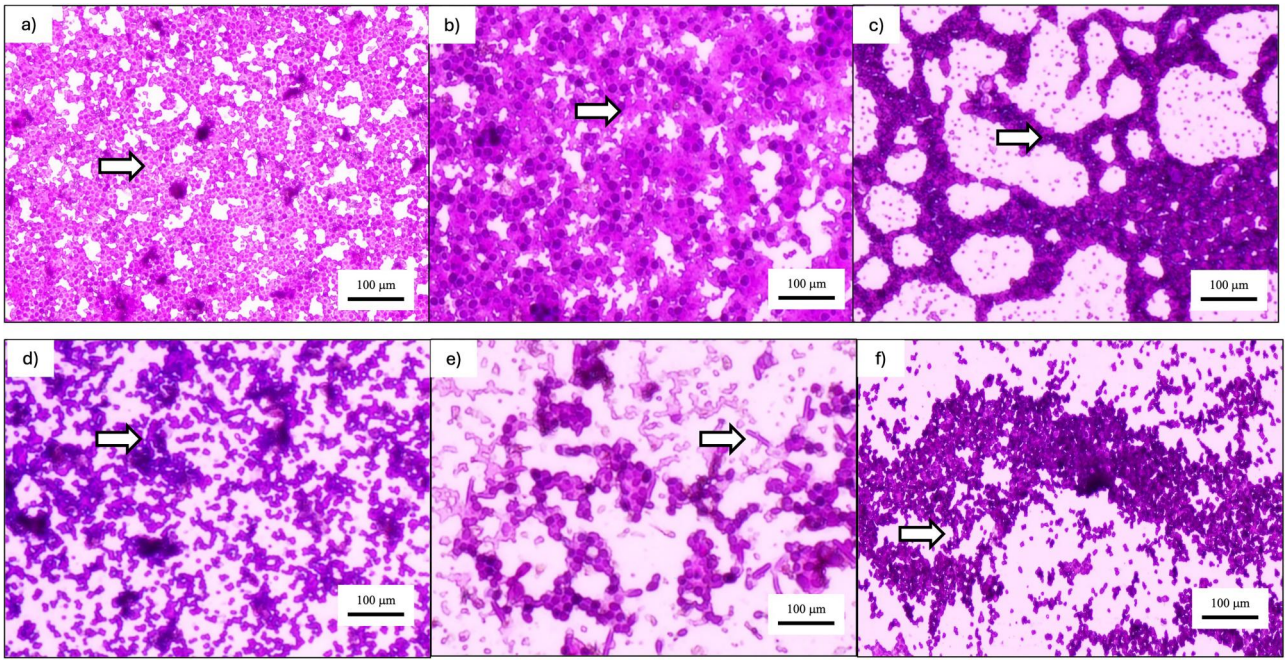

Figure 6. Photomicrographs illustrating the mono-culture biofilms of *C. auris* ATCC MYA-5002 (a), *C. albicans* ATCC MYA-4901 (b), *C. lusitaniae* ATCC 64215 (c), *C. dubliniensis* ATCC MYA-2975 (d), *C. parapsilosis* ATCC 22019 (e) and *C. glabrata* ATCC 90030 (f) at 40× magnification. Biofilms grown in RPMI-1640 for 72 h at 37 °C. The white arrows indicate the morphology of *Candida* yeast (a, b, c, d, and f) and hyphae (e).

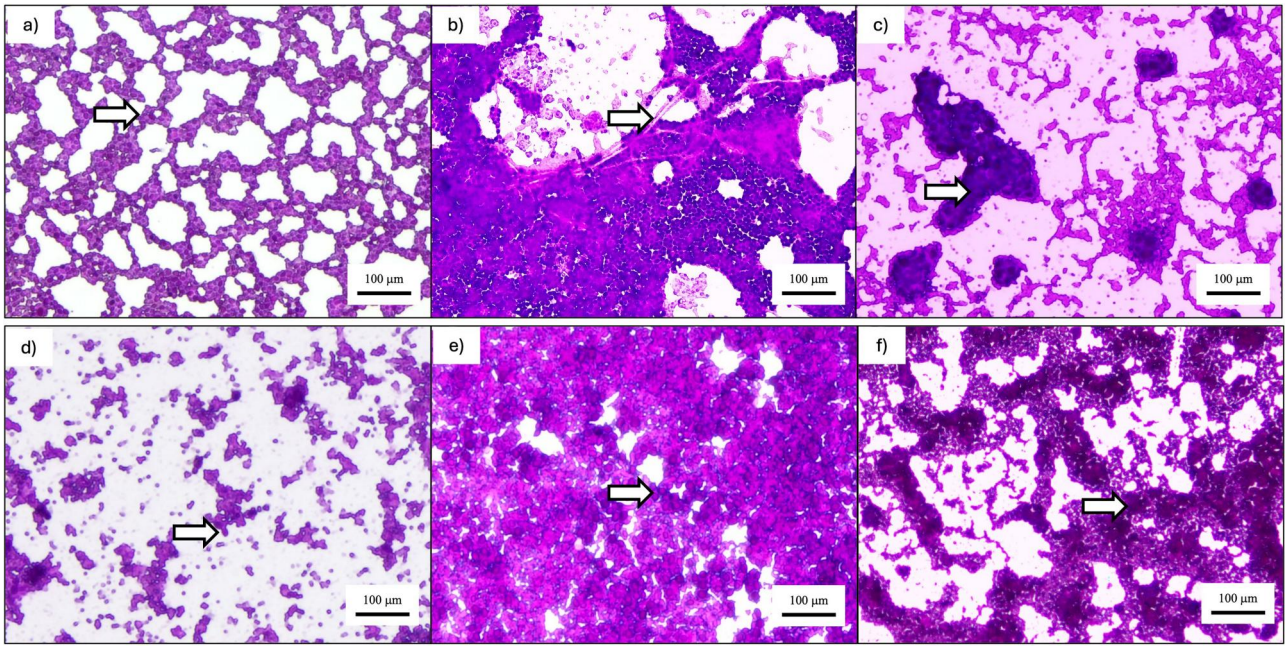

Figure 7. Photomicrographs illustrating the mono-culture biofilms of *C. auris* ATCC MYA-5002 (a), *C. albicans* ATCC MYA-4901 (b), *C. lusitaniae* ATCC 64215 (c), *C. dubliniensis* ATCC MYA-2975 (d), *C. parapsilosis* ATCC 22019 (e) and *C. glabrata* ATCC 90030 (f) at 40× magnification. Biofilms were grown in YPD for 72 h at 37 °C. The white arrows indicate the morphology of *Candida* yeast (a, c, d, e,and f) and hyphae (b).

highlights their clinical significance, establishing a foundation for understanding interkingdom interactions that contribute to the development of oral diseases. This study utilises three different media: RPMI-1640, YPD and BHIYE, which represent unique microenvironments in the oral cavity.

RPMI-1640 is a medium with a rich amino acid and low-glucose composition. It simulates nutrient-

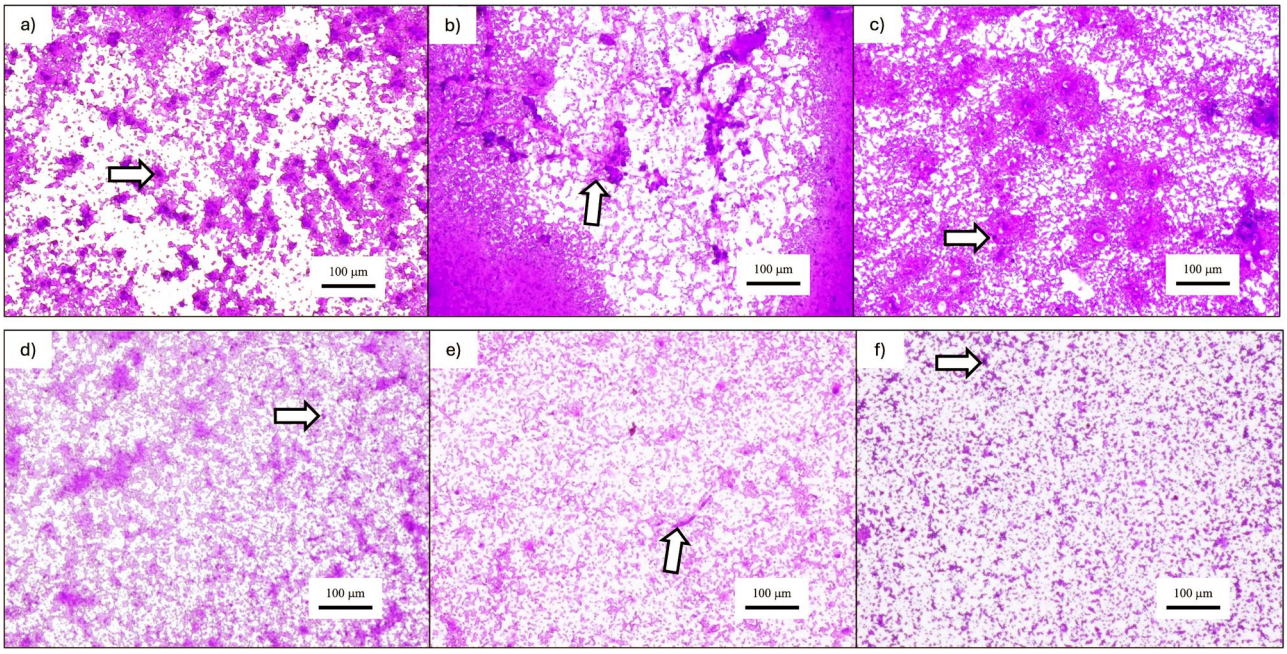

Figure 8. Photomicrographs illustrating the co-culture biofilms of *S. aureus* and *C. auris* ATCC MYA-5002 (a), *C. albicans* ATCC MYA-4901 (b), *C. lusitaniae* ATCC 64215 (c), *C. dubliniensis* ATCC MYA-2975 (d), *C. parapsilosis* ATCC 22019 (e) and *C. glabrata* ATCC 90030 (f) at 40× magnification. Biofilms grown in BHIYE for 72 h at 37 °C. The white arrows indicate the dark-stained yeast (a, c, d, e, and f) and hyphae (e) morphologies showing the encapsulation of *Candida* by *S aureus*.

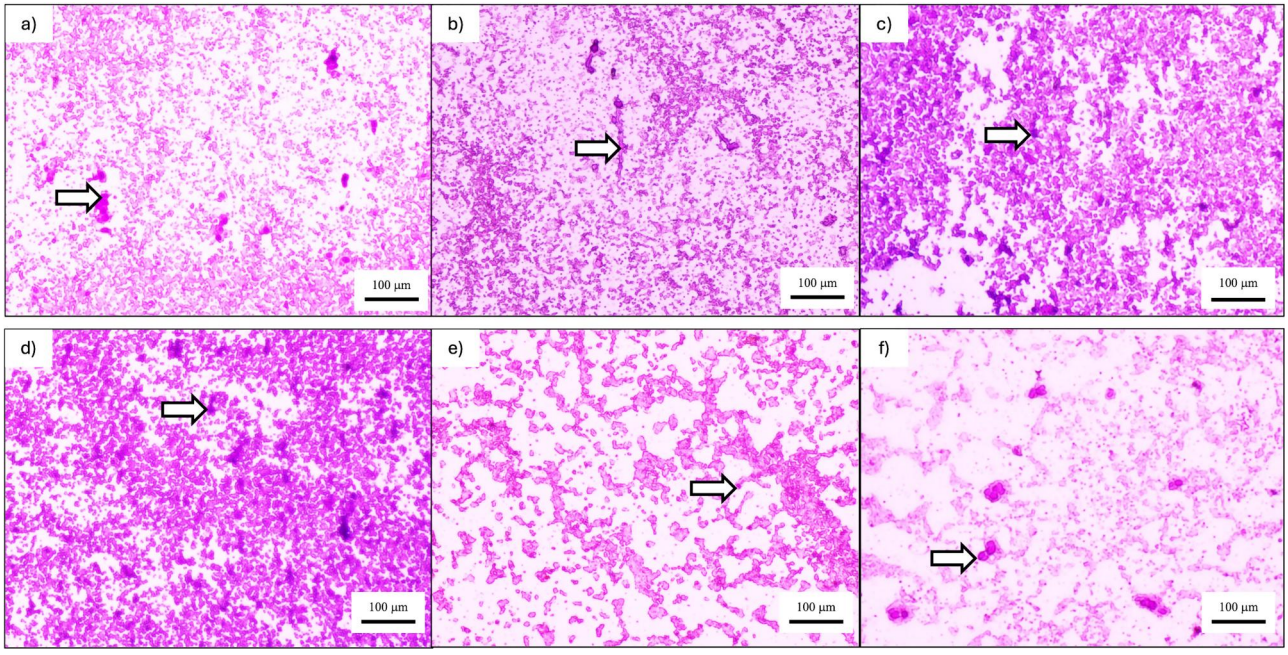

Figure 9. Photomicrographs illustrating the co-culture biofilms of *S. aureus* and *C. auris* ATCC MYA-5002 (a), *C. albicans* ATCC MYA-4901 (b), *C. lusitaniae* ATCC 64215 (c), *C. dubliniensis* ATCC MYA-2975 (d), *C. parapsilosis* ATCC 22019 (e) and *C. glabrata* ATCC 90030 (f) at 40× magnification. Biofilms grown in RPMI-1640 for 72 h at 37 °C. The white arrow indicates the dark-stained yeast (a, c, d, e, and f) and hyphae (b) morphologies showing the encapsulation of *Candida* by *S aureus*.

limited conditions of gingival crevicular fluid in periodontal pockets or subgingival regions. Thus, reduced *Candida* cell counts when in co-culture with *S. aureus* under these conditions may reflect the interkingdom interactions that are likely to occur in subgingival biofilm, where bacterial dominance could suppress fungal proliferation (Lamont et al. 2018).

Meanwhile, YPD serves as a medium that promotes fungal growth and simulates carbohydrate-rich oral environments, such as areas of dental plaque

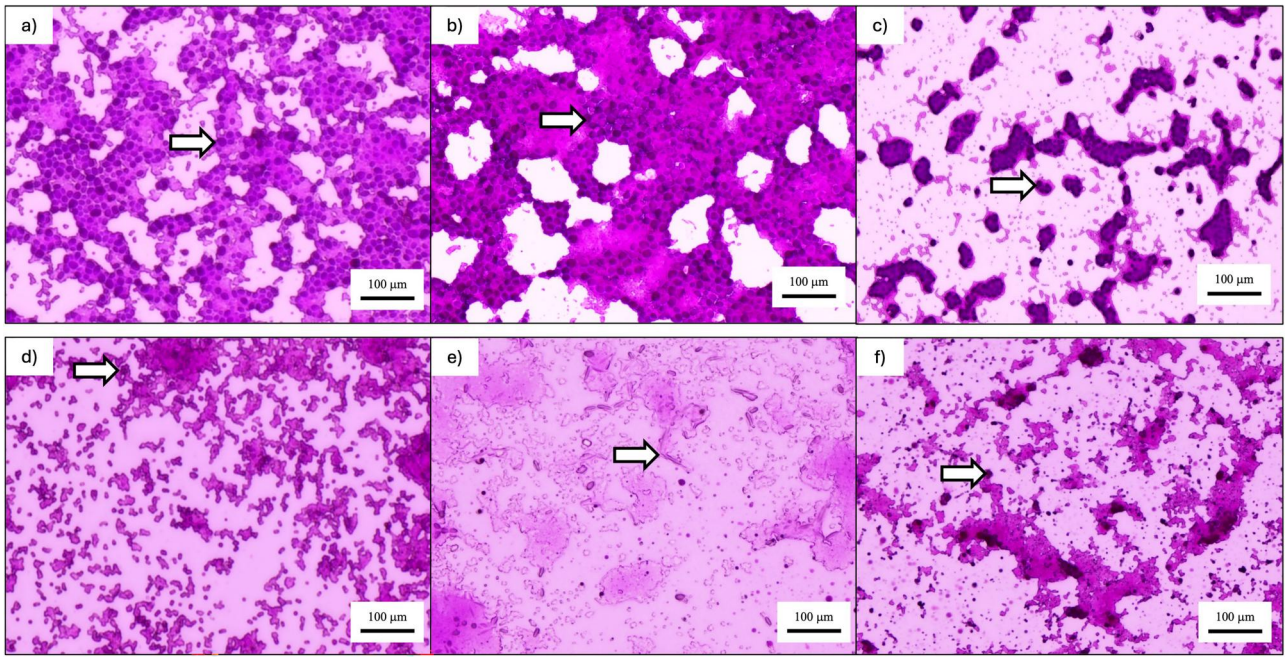

Figure 10. Photomicrographs illustrating the co-culture biofilms of *S. aureus* and *C. auris* ATCC MYA-5002 (a), *C. albicans* ATCC MYA-4901 (b), *C. lusitaniae* ATCC 64215 (c), *C. dubliniensis* ATCC MYA-2975 (d), *C. parapsilosis* ATCC 22019 (e) and *C. glabrata* ATCC 90030 (f) at 40× magnification. Biofilms grown in YPD for 72 h at 37 °C. The white arrow indicates the dark-stained yeast (a, b, c, d, and f) and hyphae (e) morphologies showing the encapsulation of *Candida* by *S aureus*.

exposed to frequent sucrose intake. The elevated biofilm biomass of *C. dubliniensis* and *C. glabrata* in YPD mono-cultures corresponds with clinical observations of *Candida* overgrowth in individuals prone to caries or patients with uncontrolled diabetes (Hwang 2022).

BHIYE, enriched with peptones and yeast extract, mimics nutrient-rich environments such as saliva-coated mucosal surfaces or supragingival plaques. The increased co-aggregation of *C. auris* or *C. albicans* with *S. aureus* in BHIYE highlights the role of salivary proteins and dietary residues that may facilitate interkingdom interactions. This synergism is clinically significant: *C. albicans*-*S. aureus* co-colonisation is implicated in refractory oral candidiasis and denture stomatitis, where biofilms evade host defences and antifungals (Van Dyck et al. 2021).

The present study showed that auto-aggregation and co-aggregation varied among *Candida* spp. across different types of media, thus supporting the hypothesis of this study that aggregation is media and species-dependent. The result in this study is consistent with a previous study that demonstrated co-aggregation between *C. albicans* and *S. aureus* depending on nutritional status and candidal morphology (Stevens et al. 2015; Montelongo-Jauregui and Lopez-Ribot 2018). RPMI-1640 contains amino acids (L-glutamine, L-arginine and L-asparagine), vitamins and inorganic salts. However, compared to YPD and BHIYE, the RPMI-1640 medium has low glucose content and lacks yeast extract (Weerasekera et al. 2016). This justifies the higher planktonic growth observed in YPD and BHIYE, which are nutrient-rich media. YPD is a selective agar for *Candida*; however, it lacks the composition of the heart and calf brain, which can improve the growth of microorganisms (Sánchez-Alonzo et al. 2020). Thus, it has been postulated that nutrients in the growth medium can influence the interkingdom interactions between fungi and bacteria in planktonic environments (Nev et al. 2021).

In addition, *C. auris* and *C. albicans* increased co-aggregation percentage when co-cultured with *S. aureus* in BHIYE, suggesting that nutrient-rich environments support strong interkingdom interactions. Thus, these findings suggest that the presence of *S. aureus* enhances the co-aggregation potential of these interkingdom species in specific environments. The composition of the growth media, including nutrient availability, pH levels and osmolarity, can substantially affect the co-aggregation of *Candida* spp. and *S. aureus* (Weerasekera et al. 2016). Different growth media provide different levels and types of nutrients. Nutrient-rich media, such as brain heart infusion enriched with yeast extract (BHIYE), support the growth of two kingdoms of microorganisms: bacteria and fungi (Zago et al. 2015; Montelongo-Jauregui and Lopez-Ribot 2018). This medium is enriched with higher levels of peptones, proteins,

B-complex vitamins and other nutrient-dense meat infusions that support growth and stimulate microbial proliferation (Moore and McMullan 2003; Basu et al. 2015). In contrast, co-aggregation is often reduced when grown in nutrient-limited media (Montelongo-Jauregui and Lopez-Ribot 2018).

The development of biofilms leads to fungal invasion and resistance, resulting in oral conditions such as oral candidiasis (Hyun Koo et al. 2018; Hwang 2022). In the present study, biofilm biomass in mono- and co-culture was found to vary between species and growth medium, thus supporting the hypothesis that biofilm formation is media and species-dependent. This present study showed that co-culture with *S. aureus* in BHIYE, resulted in higher biofilm biomass than mono-culture for *C. auris*, *C. albicans*, *C. lusitaniae* and *C. glabrata.* These findings suggest that specific interkingdom interactions between *Candida* spp. and *S. aureus* might enhance biofilm development (Konečná et al. 2021). Previous studies highlighted the synergistic relationship between *C. albicans* and *S. aureus* in developing inter-kingdom biofilms in the oral cavity (Schlecht et al. 2015; Hu et al. 2021; Van Dyck et al. 2021).

The findings from this study showed that co-culture of *C. albicans* with *S. aureus* in RPMI-1640 and BHIYE resulted in increased co-aggregation scores compared to auto-aggregation. Previous studies have highlighted the synergistic interaction between *C. albicans* or *C. auris* and *S. aureus* regarding biofilm formation and infections (Hu et al. 2021; Khan et al. 2023). This synergistic interaction includes both targeted adhesin-receptor binding and non-specific interactions. Consequently, it increases the pathogenicity of both microorganisms, resulting in more severe infections and promoting the rise of vancomycin resistance in *S. aureus* (Kean et al. 2017; Camarillo-Márquez et al. 2018; Van Dyck et al. 2021). This interkingdom interaction could lead to a complex infection resulting in an aggressive form of the disease, including increased resistance to antimicrobials that interfere with therapeutic management (Schlecht et al. 2015; Carolus et al. 2019).

A comparison of total cell counts in mono-culture versus co-culture biofilms revealed that *S. aureus* significantly reduced the total cell count of *Candida* spp. in co-culture ($p < 0.05$). The findings in the present study suggest that *S. aureus* exerts antagonistic effects on *Candida* spp. in co-culture biofilms, reducing total *Candida* cell counts across different media. The competitive interactions between *S. aureus* and *Candida* spp. observed in this study may arise due to several factors, including competition for nutrients, production of antimicrobials, pH and environmental modulation, and physical interactions (Carolus et al. 2019; Zhu et al. 2023).

These findings also suggest that *S. aureus* competes with *Candida* spp. in co-culture conditions by depleting essential nutrients such as glucose, amino acids and iron, particularly in nutrient-limited conditions like RPMI-1640. Additionally, *S. aureus* is known to produce antimicrobial factors, including bacteriocins and metabolic byproducts, which may contribute to the observed reduction in *Candida* cell counts during co-culture biofilms (Goc et al. 2023; Zhu et al. 2023). Another potential mechanism is the capability of *S. aureus* to modify the microenvironment by adjusting pH and oxygen levels, thereby creating conditions that are less conducive to *Candida* growth. Furthermore, *S. aureus* has been reported to adhere to *Candida* hyphae, which may limit fungal growth and affect biofilm formation integrity (Carolus et al. 2019; Van Dyck et al. 2021).

Moreover, the effect of growth media on microbial interactions emphasises the important role of nutrient availability in determining competitive outcomes. In BHIYE, a nutrient-rich medium supplemented with peptones, proteins, B-complex vitamins and yeast extract, certain *Candida* spp., particularly *C. auris*, *C. albicans* and *C. glabrata*, exhibited enhanced biofilm formation despite co-culture with *S. aureus*. This indicates that *Candida* spp. might be more robust against bacterial competition in nutrient-rich conditions, potentially owing to better metabolic adaptation or enhanced biofilm matrix production (Hyun Koo et al. 2018; Hwang 2022). In contrast, RPMI-1640, which contains lower glucose and lacks yeast extract, led to a significant reduction in *Candida* cell counts in co-culture, suggesting that *S. aureus* gains a competitive advantage under nutrient-limited conditions (Carolus et al. 2019). Meanwhile, YPD, optimised for fungal growth, resulted in weaker antagonistic effects from *S. aureus*, allowing for greater *Candida* biofilm biomass (Gülmez et al. 2022). These findings emphasise the importance of nutrient composition in growth media factors that may influence microbial activity in interkingdom interactions.

The media-dependent antagonism and synergism observed here provide insights into oral disease progression. For example, in periodontal pockets (analogous to RPMI-1640), bacterial competition may initially suppress *Candida*; however, dysbiosis or antibiotic use could disrupt this balance, allowing fungal introduction invasion (Carolus et al. 2019).

Meanwhile, in sucrose-rich environments (such as YPD), *Candida* may thrive independently, exacerbating enamel demineralisation and dental caries. The co-aggregation of *C. auris* and *S. aureus* in BHIYE suggests that salivary glycoproteins could enhance biofilm adhesion on mucosal surfaces, predisposing immunocompromised patients to chronic candidiasis or *Candida*-bacterial infections particularly in nosocomial settings (Gülmez et al. 2022). This study also emphasises nutrient-driven interactions, while artificial saliva models (ASM) that include mucins and electrolytes (Sánchez-Alonzo et al. 2020) play a vital role in confirming these dynamics in physiologically relevant contexts. Furthermore, *in vivo* studies studies on *Candida-S. aureus* co-colonisation under varying dietary regimes could further clarify the causal links between nutrient availability and disease severity.

Additionally, recent advancements in co-culture models emphasise the significance of medium selection for effectively mimicking interkingdom interactions. Recent studies from Kim et al. (2020) and Kim et al. (2024) demonstrated that enhanced media formulations, such as Luria-Bertani (LB) and potato dextrose broth (PDB), were used for bacteria and fungi, respectively. These media are able to enhance the growth of both bacterial and fungal species, reducing metabolic biases linked to conventional rich media. The use of such media enables more balanced and stable co-culture biofilm formation, facilitating the study of interkingdom interactions under conditions that better reflect physiological environments (Kim et al. 2020, 2024). Integrating these recent advances in future research could not only improve the accuracy of *in vitro* biofilm models but also offer deeper insights into the intricate dynamics of interkingdom interactions that are significant in clinical settings. Thus, although the present study followed established protocols, we acknowledge the continued necessity to enhance experimental models in accordance with the evolving standards in biofilm research.

In conclusion, the relationship between *Candida* spp. and *S. aureus* is highly complex and influenced by both the species involved and environmental nutrients. Aggregation and biofilm formation vary significantly among *Candida* species and across different media. BHIYE, in particular, supports stronger co-aggregation and biofilm formation, highlighting the importance of nutrients in growth media for aggregation and biofilm formation. The co-culture of *Candida* spp. with *S. aureus* reduces biofilm biomass and cell count, although certain species, like *C. auris, C. albicans* and *C. glabrata*, exhibit enhanced biofilm formation in specific growth media. Thus, these findings provide an understanding of the mechanisms underlying the cross-kingdom interactions between nosocomial pathogens *Candida* spp. and *S. aureus* in different nutrient environments and have important implications in biofilm-associated infections.

Acknowledgements

The authors would like to acknowledge the International Islamic University of Malaysia (IIUM) for the laboratory services and Universiti Teknologi MARA (UiTM) for research support.

Author contributions

CRediT: **Wan NurHazirah Wan Ahmad Kamil**: Formal analysis, Investigation, Resources, Visualization, Writing – original draft; **Mukarramah Zainal**: Investigation, Methodology; **Munirah Mokhtar**: Data curation, Investigation, Methodology, Project administration, Resources; **H. M. H. N. Bandara**: Supervision, Validation, Writing – review & editing; **Stuart G. Dashper**: Supervision, Validation, Writing – review & editing; **Mohd Hafiz Arzmi**: Conceptualization, Data curation, Funding acquisition, Supervision, Validation, Visualization, Writing – review & editing.

Disclosure statement

No potential conflict of interest was reported by the authors.

Funding

This research is funded by the Ministry of Higher Education, Malaysia (FRGS/1/2022/SKK11/UIAM/02/2).

ORCID

Mohd Hafiz Arzmi http://orcid.org/0000-0002-9470-6412

References

Arzmi MH, Kamil W, Zainal M. 2023. Chapter 2 - Monospecies and polymicrobial biofilms in static and flow environment. In: Methods in Microbiology. Vol. 53. UK: Elsevier; p. 51–66. doi: 10.1016/bs.mim.2023.05.002.

Basu S, Bose C, Ojha N, Das N, Das J, Pal M, Khurana S. 2015. Evolution of bacterial and fungal growth media. Bioinformation. 11:182–184. doi: 10.6026/97320630011182.

Bayraktar S, Duran N, Duran GG, Eryilmaz N, Aslan H, Önlen C, Özer B. 2017. Identification of medically important *Candida* species by polymerase chain reaction-restriction fragment length polymorphism analysis of the rDNA ITS1 and ITS2 regions. Indian J Med Microbiol. 35:535–542. doi: 10.4103/ijmm.IJMM_17_102.

Camarillo-Márquez O, Córdova-Alcántara IM, Hernández-Rodríguez CH, García-Pérez BE, Martínez-Rivera MA, Rodríguez-Tovar AV. 2018. Antagonistic interaction of *Staphylococcus aureus* toward *Candida glabrata* during in vitro biofilm formation is caused by an apoptotic mechanism. Front Microbiol. 9:2031. doi: 10.3389/fmicb.2018.02031.

Carolus H, Van Dyck K, Van Dijck P. 2019. *Candida albicans* and *Staphylococcus* species: a threatening twosome. Front Microbiol. 10:2162. doi: 10.3389/fmicb.2019.02162.

Chantanawilas P, Pahumunto N, Teanpaisan R. 2024. Aggregation and adhesion ability of various probiotic strains and *Candida* species: an in vitro study. J Dent Sci. 19:2163–2171. doi: 10.1016/j.jds.2024.03.016.

Cortegiani A, Misseri G, Chowdhary A. 2019. What's new on emerging resistant *Candida* species. Intensive Care Med. 45:512–515. doi: 10.1007/s00134-018-5363-x.

Di Cosola M, Cazzolla AP, Charitos IA, Ballini A, Inchingolo F, Santacroce L. 2021. *Candida albicans* and oral carcinogenesis. A brief review. J Fungi (Basel). 7:476. doi: 10.3390/jof7060476.

Deo PN, Deshmukh R. 2019. Oral microbiome: unveiling the fundamentals. J Oral Maxillofac Pathol. 23:122–128. doi: 10.4103/jomfp.JOMFP_304_18.

Deo PN, Deshmukh R. 2020. Oral microbiome and oral cancer—The probable nexus. J Oral Maxillofac Pathol. 24:361–367. doi: 10.4103/jomfp.JOMFP_20_20.

Eichelberger KR, Paul S, Peters BM, Cassat JE. 2023. *Candida*–bacterial cross-kingdom interactions. Trends Microbiol. 31:1287–1299. doi: 10.1016/j.tim.2023.08.003.

Farooq H, Monowar T, Latt S, Chinni S, Zainol N, Sabesan G. 2022. A review of studies on *Candida* species in Peninsular Malaysia. Adv Biomed Res. 11:98. doi: 10.4103/abr.abr_3_22.

Goc A, Sumera W, Rath M, Niedzwiecki A. 2023. Inhibition of α-hemolysin activity of *Staphylococcus aureus* by theaflavin 3,3'-digallate. PLoS One. 18:e0290904. doi: 10.1371/journal.pone.0290904.

Gülmez D, Brown JL, Butcher MC, Delaney C, Kean R, Ramage G, Short B. 2022. Investigating dual-species *Candida auris* and *Staphylococcal*. Antibiotics. 11:931. doi: 10.3390/antibiotics11070931.

Hu Y, Niu Y, Ye X, Zhu C, Tong T, Zhou Y, Zhou X, Cheng L, Ren B. 2021. *Staphylococcus aureus* synergized with *Candida albicans* to increase the pathogenesis and drug resistance in cutaneous abscess and peritonitis murine models. Pathogens. 10:1036. doi: 10.3390/pathogens10081036.

Huang X, Huang X, Huang Y, Zheng J, Lu Y, Mai Z, Zhao X, Cui L, Huang S. 2023. The oral microbiome in autoimmune diseases: friend or foe? J Transl Med. 21:211. doi: 10.1186/s12967-023-03995-x.

Hwang G. 2022. In it together: *candida*-bacterial oral biofilms and therapeutic strategies. Environ Microbiol Rep. 14:183–196. doi: 10.1111/1758-2229.13053.

Hyun Koo R, Andes D, Krysan DJ. 2018. *Candida–streptococcal* interactions in biofilm-associated oral diseases. PLoS Pathog. 14:e1007342. doi: 10.1371/journal.ppat.1007342.

Kean R, Rajendran R, Haggarty J, Townsend EM, Short B, Burgess KE, Lang S, Millington O, Mackay WG, Williams C, et al. 2017. *Candida albicans* mycofilms support *Staphylococcus aureus* colonization and enhances miconazole resistance in dual-species interactions. Front Microbiol. 8:258. doi: 10.3389/fmicb.2017.00258.

Khan F, Tabassum N, Jeong GJ, Jung WK, Kim YM. 2023. Inhibition of mixed biofilms of *Candida albicans* and *Staphylococcus aureus* by β-caryophyllene-gold nanoparticles. Antibiotics (Basel). 12:726. doi: 10.3390/antibiotics12040726.

Kidd SE, Abdolrasouli A, Hagen F. 2023. Fungal nomenclature: managing change is the name of the game. Open Forum Infect Dis. 10:ofac559. doi: 10.1093/ofid/ofac559.

Kim YG, Lee JH, Park JG, Lee J. 2020. Inhibition of *Candida albicans* and *Staphylococcus aureus* biofilms by centipede oil and linoleic acid. Biofouling. 36:126–137. doi: 10.1080/08927014.2020.1730333.

Kim YG, Lee JH, Kim SH, Park SY, Kim YJ, Ryu CM, Seo HW, Lee JT. 2024. Inhibition of biofilm formation in *Cutibacterium acnes*, *Staphylococcus aureus*, and *Candida albicans* by the phytopigment shikonin. Int J Mol Sci. 25:2426. doi: 10.3390/ijms25042426.

Konečná K, Němečková I, Diepoltová A, Vejsová M, Jand'ourek O. 2021. The impact of cultivation media on the in vitro biofilm biomass production of *Candida* spp. Curr Microbiol. 78:2104–2111. doi: 10.1007/s00284-021-02452-6.

Lamont RJ, Koo H, Hajishengallis G. 2018. The oral microbiota: dynamic communities and host interactions. Nat Rev Microbiol. 16:745–759. doi: 10.1038/s41579-018-0089-x.

Marcos-Zambrano LJ, Escribano P, Bouza E, Guinea J. 2014. Production of biofilm by *Candida* and non-*Candida* spp. isolates causing fungemia: comparison of biomass production and metabolic activity and development of cut-off points. Int J Med Microbiol. 304:1192–1198. doi: 10.1016/j.ijmm.2014.08.012.

Mokhtar M, Rismayuddin NAR, Mat Yassim AS, Ahmad H, Abdul Wahab R, Dashper S, Arzmi MH. 2021. *Streptococcus salivarius* K12 inhibits *Candida albicans* aggregation, biofilm formation and dimorphism. Biofouling. 37:767–776. doi: 10.1080/08927014.2021.1967334.

Montelongo-Jauregui D, Lopez-Ribot JL. 2018. *Candida* interactions with the oral bacterial microbiota. J Fungi (Basel). 4:122. doi: 10.3390/jof4040122.

Moore JE, McMullan R. 2003. Comparison of media for optimal recovery of *Candida albicans* and *Candida glabrata* from blood culture. Ir J Med Sci. 172:60–62. doi: 10.1007/bf02915247.

Nev OA, Lindsay RJ, Jepson A, Butt L, Beardmore RE, Gudelj I. 2021. Predicting microbial growth dynamics in response to nutrient availability. PLoS Comput Biol. 17:e1008817. doi: 10.1371/journal.pcbi.1008817.

Palencia SL, García A, Palencia M. 2022. Multiple surface interaction mechanisms direct the anchoring, co-aggregation and formation of dual-species biofilm between *Candida albicans* and *Helicobacter pylori*. J Adv Res. 35:169–185. doi: 10.1016/j.jare.2021.03.013.

Papon N, Courdavault V, Clastre M, Bennett RJ. 2013. Emerging and emerged pathogenic *Candida* Species: beyond the *Candida albicans* paradigm. PLoS Pathog. 9:e1003550. doi: 10.1371/journal.ppat.1003550.

Parums DV. 2022. Editorial: the World Health Organization (WHO) fungal priority pathogens list in response to emerging fungal pathogens during the

COVID-19 pandemic. Med Sci Monit. 28:e939088. doi: 10.12659/msm.939088.

Sánchez-Alonzo K, Parra-Sepúlveda C, Vega S, Bernasconi H, Campos VL, Smith CT, Sáez K, García-Cancino A. 2020. In vitro incorporation of *Helicobacter pylori* into *Candida albicans* caused by acidic pH stress. Pathogens. 9:489. doi: 10.3390/pathogens9060489.

Sati H, Carrara E, Savoldi A, Hansen P, Garlasco J, Campagnaro E, Boccia S, Castillo-Polo JA, Magrini E, Garcia-Vello P, et al. 2025. The WHO Bacterial Priority Pathogens List 2024: a prioritisation study to guide research, development, and public health strategies against antimicrobial resistance. Lancet Infect Dis. 11:S1473-3099(25)00118-5. doi: 10.1016/S1473-3099(25)00118-5.

Schlecht LM, Peters BM, Krom BP, Freiberg JA, Hänsch GM, Filler SG, Jabra-Rizk MA, Shirtliff ME. 2015. Systemic *Staphylococcus aureus* infection mediated by *Candida albicans* hyphal invasion of mucosal tissue. Microbiology (Reading). 161:168–181. doi: 10.1099/mic.0.083485-0.

Sharma S, Mohler J, Mahajan SD, Schwartz SA, Bruggemann L, Aalinkeel R. 2023. Microbial biofilm: A review on formation, infection, antibiotic resistance, control measures, and innovative treatment. Microorganisms. 11:1614. doi: 10.3390/microorganisms11061614.

Stevens MRE, Luo TL, Vornhagen J, Jakubovics NS, Gilsdorf JR, Marrs CF, Møretrø T, Rickard AH. 2015. Coaggregation occurs between microorganisms isolated from different environments. FEMS Microbiol Ecol. 91: fiv123. doi: 10.1093/femsec/fiv123.

Van Dyck K, Viela F, Mathelié-Guinlet M, Demuyser L, Hauben E, Jabra-Rizk MA, Vande Velde G, Dufrêne YF, Krom BP, Van Dijck P. 2021. Adhesion of *Staphylococcus aureus* to *Candida albicans* during co-infection promotes bacterial dissemination through the host immune response. Front Cell Infect Microbiol. 10: 624839. doi: 10.3389/fcimb.2020.624839.

Vitális E, Nagy F, Tóth Z, Forgács L, Bozó A, Kardos G, Majoros L, Kovács R. 2020. *Candida* biofilm production is associated with higher mortality in patients with candidaemia. Mycoses. 63:352–360. doi: 10.1111/myc.13049.

Weerasekera MM, Wijesinghe GK, Jayarathna TA, Gunasekara CP, Fernando N, Kottegoda N, Samaranayake LP. 2016. Culture media profoundly affect *Candida albicans* and *Candida tropicalis* growth, adhesion and biofilm development. Mem Inst Oswaldo Cruz. 111:697–702. doi: 10.1590/0074-02760160294.

Wimpenny J. 2009. Microbial metropolis. Adv Microb Physiol. 56:29–84. doi: 10.1016/S0065-2911(09)05602-1.

Zago CE, Silva S, Sanitá PV, Barbugli PA, Dias CMI, Lordello VB, Vergani CE. 2015. Dynamics of biofilm formation and the interaction between *Candida albicans* and methicillin-susceptible (MSSA) and -resistant *Staphylococcus aureus* (MRSA). PLoS One. 10:e0123206. doi: 10.1371/journal.pone.0123206.

Zhu Z, Hu Z, Li S, Fang R, Ono HK, Hu DL. 2023. Molecular characteristics and pathogenicity of *Staphylococcus aureus* exotoxins. IJMS. 25:395. doi: 10.3390/ijms25010395.